Silicon–Carbon Bond Inversions Driven by 60-keV Electrons in Graphene

Toma Susi,[1,*] Jani Kotakoski,[1,2] Demie Kepaptsoglou,[3] Clemens Mangler,[1] Tracy C. Lovejoy,[4] Ondrej L. Krivanek,[4] Recep Zan,[5,6] Ursel Bangert,[5,7] Paola Ayala,[1] Jannik C. Meyer,[1] and Quentin Ramasse[3]

[1]*Faculty of Physics, University of Vienna, Boltzmanngasse 5, A-1090 Vienna, Austria*
[2]*Department of Physics, University of Helsinki, P.O. Box 43, FI-00014 Helsinki, Finland*
[3]*SuperSTEM Laboratory, STFC Daresbury Campus, Daresbury WA4 4AD, United Kingdom*
[4]*Nion Co., 1102 8th Street, Kirkland, Washington 98033, USA*
[5]*School of Materials, The University of Manchester, Manchester M13 9PL, United Kingdom*
[6]*Department of Physics, Faculty of Arts and Sciences, Niğde University, 51000 Niğde, Turkey*
[7]*Department of Physics and Energy, University of Limerick, Limerick, Ireland*

We demonstrate that 60-keV electron irradiation drives the diffusion of threefold-coordinated Si dopants in graphene by one lattice site at a time. First principles simulations reveal that each step is caused by an electron impact on a C atom next to the dopant. Although the atomic motion happens below our experimental time resolution, stochastic analysis of 38 such lattice jumps reveals a probability for their occurrence in a good agreement with the simulations. Conversions from three- to fourfold coordinated dopant structures and the subsequent reverse process are significantly less likely than the direct bond inversion. Our results thus provide a model of nondestructive and atomically precise structural modification and detection for two-dimensional materials.

Recent breakthrough developments in imaging and spectroscopy in (scanning) transmission electron microscopy [(S)TEM] have enabled the study of structural modifications that occur very literally at the atomic scale. Because of their low dimensionality, materials such as carbon nanotubes, and especially graphene, have proven ideal for these investigations [1–6]. At the same time, (S)TEM instruments can also be turned into nanosculpting tools: for example, graphene ribbons with specific geometries [7], or perforations of controlled sizes [8,9], can be fabricated via adjustments of the local chemistry, electron beam energy, and density. Heteroatom doping is another way to tailor the properties of graphene [10], which is otherwise ill suited for many applications due to its lack of an electronic band gap [11]. Exchanging some of the carbon atoms by boron or nitrogen can result in an opening of the gap [12,13], while localized enhancements of plasmon resonances can be created around single silicon substitutions, which then act as atomic antennas [14]. The ability to directly observe the effect of single dopants is thus of the utmost importance in the further development of nanoengineering.

However, doping changes the effect an electron beam has on the atomic structure of graphene, as we have recently shown for nitrogen substitutions [15]. In that case, the slightly higher mass of nitrogen as compared to carbon leads to an increased likelihood to knock out the carbon atoms next to the dopant rather than the dopant itself or C in pristine areas. We also predicted that damage would be negligible at a primary beam energy of 60-keV, which was recently confirmed by atomic resolution imaging and electron energy loss spectroscopy (EELS) [2,3]. Recent studies established that silicon dopants—significantly heavier and larger in covalent radius than either carbon or nitrogen—can bond in two distinct ways within the lattice: a nonplanar, threefold-coordinated configuration (denoted Si-C_3) where the Si atom replaces a single carbon atom, binding to three neighboring C and buckles out of the graphene plane; and a planar, fourfold coordinated configuration (Si-C_4), where the Si atom is bonded to four C atoms and occupies a divacancy in the lattice [4,5]. Although beam damage was occasionally observed, apart from a study on the dynamics of Si_6 clusters in a graphene pore [16], the effects of electron irradiation have not been reported in detail.

In this Letter, we show that structural changes in silicon-doped graphene (Si-graphene) drastically differ from those in nitrogen-doped graphene. For Si-graphene, they predominantly take the form of a random walk by the Si atoms through the lattice, with no other changes in the structure. Through first-principles molecular dynamics simulations, we show that each step is a result of an electron impact on one of the C atoms neighboring the Si, and how the non-planarity of the structure plays a crucial role. The probability calculated for this process agrees well with an estimate obtained through a stochastic analysis of the experimental data. We further discuss the few observed

events that lead to the conversion of Si-C_3 sites into Si-C_4 ones, and show that they are well accounted for as knock-on damage. The significantly greater probability of the nondestructive reorganization coupled with its directionality should allow the motion of the Si atoms to be controlled with atomic precision.

Our graphene samples were synthesized by chemical vapor deposition [17], and typically contain a low concentration of silicon incorporated as individual dopants in the lattice [4,5,18]. We observed the samples using a Nion UltraSTEM™ 100 electron microscope equipped with a cold field emission gun operated at a 60-keV primary beam energy in near-ultrahigh vacuum (2×10^{-7} Pa) [5,19]. The Si atoms can be directly identified within STEM images by their brighter contrast with respect to the graphene lattice C atoms due to their higher atomic number [20]. The identification has also been verified by atomically resolved EELS [4,5].

In Fig. 1, we illustrate the predominant beam-induced process, whereby the Si atom is seen to move from one lattice site to the next during continuous imaging with an estimated dose rate of 2.2×10^7 $e^-/\text{Å}^2$ s. Since atomic motion happens at subpicosecond time scales, electron microscopy can only capture static snapshots of structures that are in effect fully relaxed. Although processes happening below our experimental time resolution of 88 ms cannot be ruled out, our observations give us a high degree of confidence that we capture the relevant dynamics. The observed events are nondestructive reorganizations of the structure, similar to the process of Stone-Wales transformations that were earlier shown to be due to subthreshold electron impacts [21], rather than thermally driven bond rotations [22]. The process is
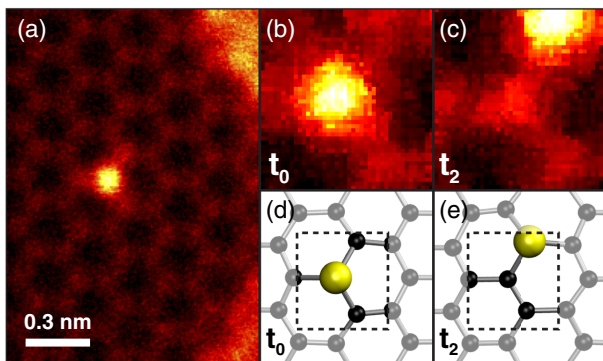
also not limited to perfect hexagonal arrangements (see the Supplemental Material [23]).

To gain insight into the dynamics of such processes at the atomic scale, we used density functional theory molecular dynamics (DFT MD) calculations as described in more detail in Refs. [15,21,24]. Although DFT describes the electronic ground state, the atomic dynamics take place over tens to hundreds of femtoseconds, whereas the relevant electron dynamics occur on sub-fs time scales in a metallic system [25]. Ionization effects were also explicitly ruled out by experiments with ^{12}C and ^{13}C graphene [26]. Thus, the ground state approximation is valid to a good degree of accuracy. In high-energy irradiation, the displacement threshold T_d is defined as the minimum kinetic energy required by an atom to be removed from its position in a material. We estimated it by increasing the starting kinetic energy of a target atom until it escaped the structure during the course of an MD simulation. For atomic rearrangements, the same procedure was used to establish threshold limits for a particular reorganization.

The calculations were performed using the grid-based projector-augmented wave code (GPAW [27,28]; for details on the computational parameters see Ref. [23]). To speed up the calculations, we used a double-zeta linear combination of atomic orbitals (LCAO) basis. However, we directly compared the calculated knock-on thresholds for C in pristine graphene and the Si atom in Si-graphene with our earlier methodology [29,30], and established agreement within our computational accuracy. Furthermore, we double checked the Si jump threshold by full accuracy finite-differences calculations.

The nonplanar Si-C_3 configuration can have two distinct positions with respect to the beam direction: the Si atom either protrudes "below" (in the instrument geometry) the plane towards the incoming beam, or "above" it along the direction of the beam. These present different T_d and cannot be experimentally distinguished from a two-dimensional projection of the lattice recorded with a normally incident beam. However, we suspected that the threshold for flipping a Si atom from below to above should not be very high even for 60-keV electrons, as no bonds need to be broken for the transformation. Indeed, a nudged elastic band [31] calculation yields a barrier of only ca. 1.1 eV for this process (see Ref. [23]). Thus, all Si configurations are effectively above the graphene plane under observation, and the beam-induced alignment is expected to be thermally stable.

Our simulations yield a T_d of approximately 13.25 eV for the Si atom bonded in the Si-C_3 configuration. However, due to the large mass of Si (28 amu), the probability for 60-keV electrons to transfer this much energy to the dopant is low, resulting in a cross section of 6.6×10^{-7} b when out-of-plane lattice vibrations with a Debye temperature of 1287 K are taken into account [26]. This agrees well with the observation that Si atoms are rarely lost [4,5,16]. The knock-on threshold for one of the three C neighbors
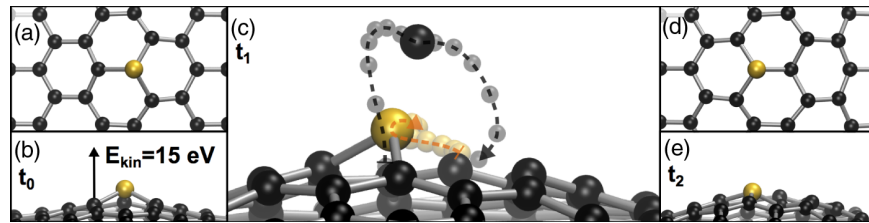

FIG. 1 (color online). (a) An area of graphene where the bright contrast originates from a single Si-C_3 dopant [high-angle annular dark field (HAADF) detector]. (b) A closer view of a Si site under continuous 60-keV electron irradiation in a reduced scan window at time t_0 [binned over six exposures of 88 ms, medium-angle annular dark field (MAADF) detector]. (c) The same area, one binned frame (0.5 s) later at time t_2, where the Si atom is observed to have moved by one lattice site (MAADF). (d),(e) Structural models where the areas shown in (b),(c) are outlined by the dashed lines.

FIG. 2 (color online).   Molecular dynamics simulation of an electron impact delivering 15 eV to a C atom neighboring Si-C_3 in graphene. (a) Top view of the starting configuration at time t_0. (b) Side view at t_0, with the kinetic energy indicated on the impacted atom. (c) A snapshot at t_1 (~700 time steps into the simulation), with the entire trajectories of the ejected C atom and the Si atom marked by semitransparent balls and dashed lines. (d) Top view near the end of the simulation at time t_2 after ~1400 time steps. (e) Side view at time t_2. Note that although the atomic motion has not ceased by this point, no further changes in the atomic configuration follow.

to Si is higher, about 16.875 eV, but leads to a much larger cross section (~0.022 b) due to the lower mass of C (unless otherwise stated, we refer to ^{12}C). This process leads to a conversion Si-C_3 → Si-C_4, which can occur at high irradiation doses.

More interesting are impacts below T_d, which nevertheless lead to local changes in the structure. For example, energies between 15.0 and 16.25 eV result in the C atom being ejected from the lattice, but with a trajectory curving first slightly away and then towards the Si due to their mutual interaction. The Si simultaneously relaxes towards the vacated lattice site, as illustrated for the 15 eV case in Fig. 2 (a movie is available through Ref. [23]). Between 16.5 to 16.75 eV the C atom almost escapes, but is drawn back by the attractive interaction with the Si atom to land on top of the lattice on the side opposite to its starting position, while the remaining structure assumes the Si-C_4 configuration. At 14.5 eV, the ejected C is left as an adatom directly to the side of the Si, but at 14.75 eV, it bounces off the Si atom on its downward trajectory and lands as an adatom on the opposite side. For energies below 14.5 eV, no change in the structure is obtained.

Because Si-C_3 is energetically favored over Si-C_4 (by ca. 1.02 eV [23]), it is likely that all configurations where the C adatom remains very close will relax back into the Si-C_3 configuration (whether this results in an apparent jump event likely depends on whether C landed on the opposite side). We thus take 14.625 eV to be the lower threshold for this process, corresponding to a cross section of 0.494 b. To estimate the cross section for moving the Si dopant, we subtract the cross section corresponding to T_d (as the largest cross section is a sum of the cross sections of all possible outcomes), i.e., $0.494 - 0.022 = 0.472$ b. If we instead assume no recombination of C adatoms with the Si-C_4 site, the cross section estimate is reduced to 0.316 b. (These would be 0.130 and 0.084 b for ^{13}C, respectively.) All of the reported results correspond to displacements in a direction perpendicular to the graphene plane, and the curved trajectory is a result of the silicon–carbon interaction.

To double check the calculated values, we carried out a few computationally demanding simulations using the default GPAW finite differences (FD) mode. The FD calculations gave a slightly lower knock-on threshold of 16.625 eV (0.032 b), but also a lower flip threshold of 14.375 eV (0.666 b); the jump cross section would thus be $0.666 - 0.032 = 0.634$ b [32].

In our experimental data, we found 38 cases where a clear Si jump was observed, with one continuous time series containing 19 consecutive jumps of the same Si atom (Fig. 3). The event doses (i.e., the irradiation doses between structural rearrangements) determined for the centre of the scan area ranged from 0.24 to 20.01×10^8 $e^-/Å^2$. However, as the scan frame was centred on the Si atom, the doses on the neighboring carbon atoms varied from scan to scan, which was taken into account via a Monte Carlo integration. If we assume that the data are stochastic, the waiting times (or, equivalently, the doses) should be Poisson distributed.
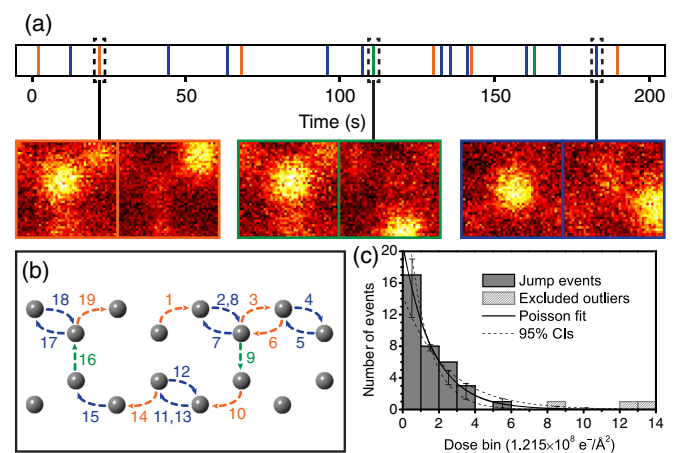

FIG. 3 (color online).   (a) An experimental time series of 19 consecutive jumps. Vertical lines mark the observed times of the jumps from the beginning of the experiment. Each event has a color corresponding to one of the three inequivalent bonds in the lattice over which the jump occurred. Insets: micrographs showing the third, ninth, and 18th jump events (MAADF detector, each binned from six consecutive 88 ms frames). (b) A schematic illustration of the directions of the jumps in the lattice. (c) A histogram of the observed event doses with the optimized bin width [23]. The solid line is an exponential with the fitted Poisson mean. The excluded outliers are shown in light gray (see text).

Thus, the expected value of a Poisson distribution fitted to the data can be used to estimate a cross section for the process (see Ref. [23] for details).

We obtained an expectation value of 2.57×10^8 $e^-/\text{Å}^2$ for the event dose, with a 95% confidence interval (CI$_{95\%}$) of $[1.59, 4.09] \times 10^8$ $e^-/\text{Å}^2$ [33]. This yields an interaction cross section of 0.389 b (CI$_{95\%}$ [0.244, 0.629] b). However, further comparison between the data and the obtained Poisson distribution reveals that three events with the highest doses have a probability lower than 10^{-3} to be a result of the same process. We believe that some of these can be due to ^{13}C atoms incorporated into the graphene lattice (1.1% of all C atoms can be expected to be ^{13}C), or due to a combination of either a jump and an immediate reverse jump or a displacement and refill by an adatom. Reanalysis of the data without the outliers results in a revised expectation value of 1.63×10^8 $e^-/\text{Å}^2$ (CI$_{95\%}$ $[1.12, 2.37] \times 10^8$ $e^-/\text{Å}^2$), and a corresponding interaction cross section of 0.613 b (CI$_{95\%}$ [0.423, 0.893] b) [34].

The experimental value is in remarkably good agreement with the FD calculation (0.634 b), and within its CI$_{95\%}$ also with the range of [0.316, 0.472] b estimated from the more extensive LCAO simulations. Figure 3(c) shows a histogram of the event doses, which—as expected for a Poisson process—are found to be well described by an exponential with the fitted Poisson mean (apart from an excess of one event in the third bin, and a deficit of one event in the fifth).

Our data also contains eight events where Si-C$_3$ is transformed into Si-C$_4$ (see Fig. 4). Taking into account the total experimental dose on trivalent sites (9.71×10^9 $e^-/\text{Å}^2$), we get an estimated cross section of 0.08 b for this process, in good agreement with the calculated value of 0.066 b [35]. Interestingly, the knock-on threshold for the four C neighbors of the Si-C$_4$ was calculated to be 17.125 eV, i.e., slightly
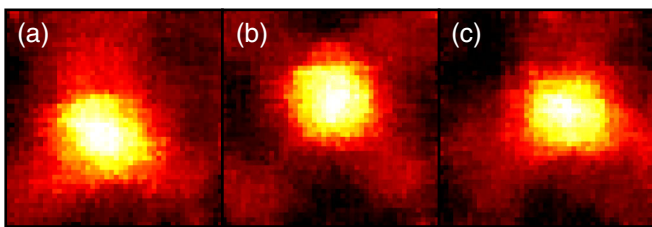

FIG. 4 (color online). An example of Si-C$_3$ converting into Si-C$_4$ and back under 60-keV electron irradiation (HAADF). Frames processed with a Kuwahara noise-reduction filter (5×5 kernel), each an average of six 156 ms frames. The dose rate was estimated to be 2.8×10^7 $e^-/\text{Å}^2$s. (a) The starting configuration showing the Si atom bonded to three neighbors. (b) The same area after three binned frames (2.8 s). A single carbon atom has been removed from the site up from the Si in the image, and the Si has relaxed into fourfold coordination with four carbon neighbors. (c) In the final configuration, the site has reconverted to threefold coordination (after a further three binned frames).

higher than that for the threefold site, suggesting that Si-C$_4$ is more stable towards knock-on damage than Si-C$_3$. Indeed, a fourfold site was only once observed to damage further by the loss of atoms.

Instead, each remaining Si-C$_4$ site converted back into Si-C$_3$ with the addition of a carbon atom (see Fig. 4), presumably by adatom diffusion [36,37] and subsequent recombination into the more stable configuration. Under the nonequilibrium conditions of our experiment, the average lifetime of the Si-C$_4$ configuration was ca. 70.0 s before recombination. To understand this process, we performed additional structural relaxation simulations of Si-C$_4$ sites with a single C adatom initially bonded to C-C bridge sites 1–4 bonds away from the Si. We found the total energy of the system with the C adatom at the closest site was ~2.3 eV lower than when the C was three or four bonds away (see Ref. [23] for details). This suggests that there is an attractive force drawing in mobile adatoms into the Si-C$_4$, possibly contributing to driving the observed recombinations.

Although our analysis relied on the stochastic nature of events when all the area around the Si dopants was irradiated, it should be stressed that due to the ca. 1-Å beam diameter in modern 60-keV aberration-corrected instruments, it is possible to restrict the irradiation to a chosen carbon atom. For example, we estimate that a 1.1-Å beam with a Gaussian profile, centred on a selected C neighbor of the dopant would deposit < 0.3% of the irradiation dose on the other two C neighbors. Thus the motion of silicon atoms in the lattice can, in principle, be controlled with atomic precision. To explore this idea, we calculated the total energies of systems with two Si atoms separated by 1–4 lattice sites, and found that the energies were lower for closer separations. Remarkably, we once also experimentally observed two Si dopants moving under electron irradiation from two sites' separation to become nearest neighbors (see Ref. [23]).

To conclude, we demonstrated how 60-keV electron irradiation causes structural rearrangements at silicon dopant sites in the graphene lattice. Despite appearances, the Si atoms themselves are not perturbed by the electron beam, but undergo a random walk in the lattice due to structural relaxation taking place during a subthreshold electron impact on a neighboring carbon atom. The position of this carbon atom thus determines the direction of the walk. Therefore, restricting intense dosing only to a desired carbon atom should allow the motion of the Si atoms to be controlled with atomic precision, and arbitrary arrangements of several Si could plausibly be attained.

---

*toma.susi@univie.ac.at; toma.susi@iki.fi

[1] J. C. Meyer, C. Kisielowski, R. Erni, M. D. Rossell, M. F. Crommie, and A. Zettl, Nano Lett. **8**, 3582 (2008).

[2] U. Bangert, W. Pierce, D. M. Kepaptsoglou, Q. Ramasse, R. Zan, M. H. Gass, J. A. Van den Berg, C. B. Boothroyd, J. Amani, and H. Hofsäss, Nano Lett. **13**, 4902 (2013).

[3] R. J. Nicholls, A. T. Murdock, J. Tsang, J. Britton, T. J. Pennycook, A. Koós, P. D. Nellist, N. Grobert, and J. R. Yates, ACS Nano **7**, 7145 (2013).

[4] W. Zhou, M. D. Kapetanakis, M. P. Prange, S. T. Pantelides, S. J. Pennycook, and J.-C. Idrobo, Phys. Rev. Lett. **109**, 206803 (2012).

[5] Q. M. Ramasse, C. R. Seabourne, D.-M. Kepaptsoglou, R. Zan, U. Bangert, and A. J. Scott, Nano Lett. **13**, 4989 (2013).

[6] K. Suenaga and M. Koshino, Nature (London) **468**, 1088 (2010).

[7] Q. Xu, M.-Y. Wu, G. F. Schneider, L. Houben, S. K. Malladi, C. Dekker, E. Yucelen, R. E. Dunin-Borkowski, and H. W. Zandbergen, ACS Nano **7**, 1566 (2013).

[8] Q. M. Ramasse, R. Zan, U. Bangert, D. W. Boukhvalov, Y.-W. Son, and K. S. Novoselov, ACS Nano **6**, 4063 (2012).

[9] S. C. O'Hern, M. S. H. Boutilier, J.-C. Idrobo, Y. Song, J. Kong, T. Laoui, M. Atieh, and R. Karnik, Nano Lett. **14**, 1234 (2014).

[10] H. Terrones, R. Lv, M. Terrones, and M. S. Dresselhaus, Rep. Prog. Phys. **75**, 062501 (2012).

[11] A. H. Castro Neto, F. Guinea, N. M. R. Peres, K. S. Novoselov, and A. K. Geim, Rev. Mod. Phys. **81**, 109 (2009).

[12] D. Usachov, O. Vilkov, A. Grüneis, D. Haberer, A. Fedorov, V. K. Adamchuk, A. B. Preobrajenski, P. Dudin, A. Barinov, M. Oehzelt, C. Laubschat, and D. V. Vyalikh, Nano Lett. **11**, 5401 (2011).

[13] Y.-B. Tang, L.-C. Yin, Y. Yang, X.-H. Bo, Y.-L. Cao, H.-E. Wang, W.-J. Zhang, I. Bello, S.-T. Lee, H.-M. Cheng, and C.-S. Lee, ACS Nano **6**, 1970 (2012).

[14] W. Zhou, J. Lee, J. Nanda, S. T. Pantelides, S. J. Pennycook, and J.-C. Idrobo, Nat. Nanotechnol. **7**, 161 (2012).

[15] T. Susi, J. Kotakoski, R. Arenal, S. Kurasch, H. Jiang, V. Skalakova, O. Stephan, A. V. Krasheninnikov, E. I. Kauppinen, U. Kaiser, and J. C. Meyer, ACS Nano **6**, 8837 (2012).

[16] J. Lee, W. Zhou, S. J. Pennycook, J.-C. Idrobo, and S. T. Pantelides, Nat. Commun. **4**, 1650 (2013).

[17] X. Li, W. Cai, J. An, S. Kim, J. Nah, D. Yang, R. Piner, A. Velamakanni, I. Jung, E. Tutuc, S. K. Banerjee, L. Colombo, and R. S. Ruoff, Science **324**, 1312 (2009).

[18] T. C. Lovejoy, Q. M. Ramasse, M. Falke, A. Kaeppel, R. Terborg, R. Zan, N. Dellby, and O. L. Krivanek, Appl. Phys. Lett. **100**, 154101 (2012).

[19] Beam convergence semiangle was 31 mrad and beam current 60 pA, resulting in an estimated probe size (FWHM) of 1.1-Å. Semiangular ranges for the HAADF and MAADF detectors were 86–190 and 55–85 mrad, respectively.

[20] O. L. Krivanek, M. F. Chisholm, V. Nicolosi, T. J. Pennycook, G. J. Corbin, N. Dellby, M. F. Murfitt, C. S. Own, Z. S. Szilagyi, M. P. Oxley, S. T. Pantelides, and S. J. Pennycook, Nature (London) **464**, 571 (2010).

[21] J. Kotakoski, J. C. Meyer, S. Kurasch, D. Santos-Cottin, U. Kaiser, and A. V. Krasheninnikov, Phys. Rev. B **83**, 245420 (2011).

[22] L. Li, S. Reich, and J. Robertson, Phys. Rev. B **72**, 184109 (2005).

[23] See Supplemental Material at http://link.aps.org/supplemental/10.1103/PhysRevLett.113.115501 for details of the simulations, for structural models and details of the total energy calculations, a description of the statistical analyses along with a Wolfram Computable Document Format (http://www.wolfram.com/cdf-player/) Mathematica script and the corresponding Mathematica notebook file, electron micrographs showing two Si atoms moving closer in the lattice and a Si jump in a graphene grain boundary, and a movie of the simulated Si jump process.

[24] J. Kotakoski, D. Santos-Cottin, and A. V. Krasheninnikov, ACS Nano **6**, 671 (2012).

[25] R. Egerton, Ultramicroscopy **127**, 100 (2013).

[26] J. C. Meyer, F. Eder, S. Kurasch, V. Skakalova, J. Kotakoski, H. J. Park, S. Roth, A. Chuvilin, S. Eyhusen, G. Benner, A. V. Krasheninnikov, and U. Kaiser, Phys. Rev. Lett. **108**, 196102 (2012).

[27] J. J. Mortensen, L. B. Hansen, and K. W. Jacobsen, Phys. Rev. B **71**, 035109 (2005).

[28] J. Enkovaara et al. J. Phys. Condens. Matter **22**, 253202 (2010).

[29] G. Kresse and J. Furthmüller, Comput. Mater. Sci. **6**, 15 (1996).

[30] G. Kresse and J. Furthmüller, Phys. Rev. B **54**, 11 169 (1996).

[31] G. Henkelman and H. Jónsson, J. Chem. Phys. **113**, 9978 (2000).

[32] The FD mode should, in principle, give more accurate forces than the LCAO mode, but the inherent inaccuracy in the numerical integration of the equations of motion in the MD algorithm may render this irrelevant for the actual simulated trajectories. Thus, the different values could also be interpreted as an estimate for the inaccuracy of the calculations.

[33] M. Khamkong, Open J. Stat. **2**, 204 (2012).

[34] Our average dose per event was $2.55 \times 10^8 \, e^-/\text{Å}^2$, geometrical mean $1.22 \times 10^8 \, e^-/\text{Å}^2$. These would have resulted in estimated cross sections of 0.392 and 0.820 b.

[35] 0.096 b for the T_D from the FD calculation.

[36] Y. Gan, J. Kotakoski, A. V. Krasheninnikov, K. Nordlund, and F. Banhart, New J. Phys. **10**, 023022 (2008).

[37] R. Zan, Q. M. Ramasse, U. Bangert, and K. S. Novoselov, Nano Lett. **12**, 3936 (2012).